POSSIBLE LITHOLOGICAL TYPES AND SCIENTIFIC SIGNIFICANCE OF THE SAMPLE TO BE RETURNED BY CHANG'E-6 MISSION. X. Wang[1], J. W. Head[2], Y. Qian[3], W. Zhao[2], J. Liu[4], Y. Gao[1] and B. Wu[1]. [1]Planetary Remote Sensing Laboratory, The Hong Kong Polytechnic University, Hong Kong SAR (shane-xing.wang@polyu.edu.hk). [2]Department of Earth, Environmental and Planetary Sciences, Brown University, Providence, RI, USA. [3]Department of Earth Sciences, The University of Hong Kong, Hong Kong SAR. [4]Key Laboratory of Lunar and Deep Space Exploration, National Astronomical Observatories, Chinese Academy of Sciences, Beijing, China.

Introduction: China's next lunar exploration mission, Chang'E-6 (CE-6), is scheduled to return the first-ever samples from the enigmatic lunar farside in mid-2024. The CE-6 candidate landing sites are located at the southern part of the Apollo basin, within the ancient South Pole-Aitken (SPA) basin [1]. Three subregions were further divided, including F, L and B (Fig. 1) [1]. The CE-6 candidate landing sites involve two geological units within SPA, the Apollo basin and the central South Pole-Aitken compositional anomaly (SPACA) defined by [2]. Compared to CE-5, the samples collected by CE-6 could be more diverse in the lithological types due to the more complex geological contexts. To provide a framework for future laboratory works, here we present a preliminary predication about the materials that could be sampled by CE-6 and the associated geologic issues that could be addressed by these samples based on our current studies on the geology of the landing sites.

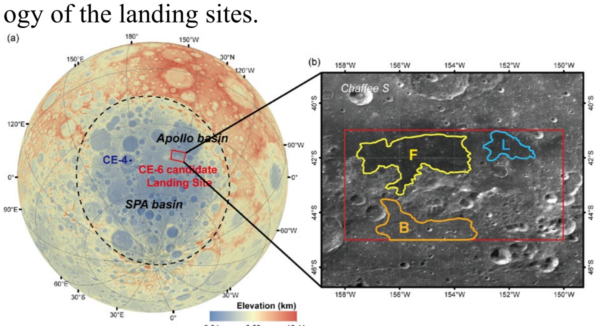

Fig. 1 The location of CE-6 candidate landing sites. (a) Topographic map of SPA basin from SLDEM2015 (+LOLA) [3]. (b) The CE-6 landing zone and the three separate subregions overlain on the CE-2 DOM map [4].

Geological Settings: The 492 km diameter Apollo peak-ring basin is located in the NE corner of the SPA basin [5]. The age of Apollo is estimated to be 3.98+0.04/-0.06 Ga [6]. The entire basin is generally anorthositic but composed of more mafic materials compared with other highland basins [7]. Within the basin interior, SW-NE compositional variations can be observed [8] and are closely correlated with local variations in crustal thickness [9]. In particular, the material exposed in the SW (including the peak ring), where the crust is thin, shows a distinctive lithology of Mg-rich noritic anorthosite, which is interpreted to have likely originated from local lunar lower crust rather than upper mantle [8]. In terms of the thorium (Th) distribution, in addition to overall decrease in Th abundance of the Apollo basin, the areas with exposure of Mg-rich noritic anorthosite show a further localized decrease in Th abundance (<2 ppm).

The Apollo basin floor is partially flooded by mare basalts. Subregions F and L belong to the Apollo southern mare region, which may have been deposited as high-Ti and low-Ti basalts during multiple periods [1]. Recent dating results suggest that F and L have different ages, and the age of F may even be as young as 2.4 Ga [1].

Subregion B is a portion of SPACA, an intermediate-albedo terrain showing pervasive elevated Ca, Fe-rich pyroxene abundance [2]. Wang et al. [10] suggest that the central region of the SPA basin has experienced widespread, post-basin resurfacing events, and interpret SPACA to have originated from more extensive cryptomaria deposits in the basin center rather than a differentiated SPA impact melt sheet. For subregion B, adjacent to the Apollo southern rim, the relatively flat surface further indicates that the resurfacing cryptomaria should have occurred in this region and covered the ejecta blanket of the Apollo basin [10].

Exotic Materials in the Landing Sites: In addition to the local mare basalts, it is highly probable that CE-6 will collect some amounts of exotic materials, which will expand the studies of the CE-6 samples. Among the three subregions, F could be the most favorable area for landing. Here we only show the preliminary investigation of the exotic materials in subregion F. Crater size-frequency distribution (CSFD) measurement shows that F has a possible young age of 2.4 Ga [1]. We look for the possible sources of foreign ejecta on the geologic map compiled by [6, 11]. We find that most craters in the surrounding units are older than F, and only Copernican-aged Chaffee S could be the main contributor of exotic materials to the subregion F.

Basic Characteristics of Chaffee S: Chaffee S is on the NW of subregion F, and its impact rays and secondaries can be clearly observed within F (Fig. 2a). Basic characteristics of Chaffee S are displayed in Fig. 2. Overall, the material excavated by Chaffee S is associated with the Mg-rich noritic anorthosite pervasively exposed in the SW interior of the Apollo basin, but differs in that it displays relatively high Th abundance. We attribute this difference to possible re-excavation of the Th-rich Oppenheimer ejecta deposit by Chaffee S. Oppenheimer is younger than Apollo [6, 11], and inevitably excavated and ejected the original Th-rich SPA basin materials onto the western interior of the Apollo basin. Subsequent excavation by the young Chaffee S exposed Oppenheimer ejecta deposits on the lunar surface, along with the Apollo basin materials.

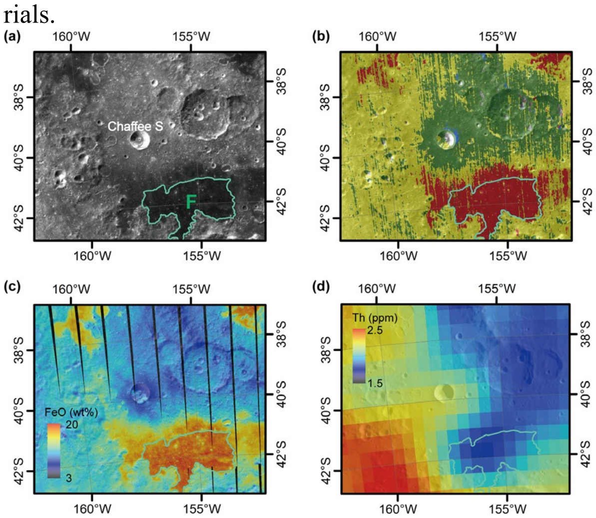

Fig. 2 *Basic characteristics of Chaffee S. (a) CE-2 DOM map [4]; (b) Spectral classification map adopted from Fig. 1b in [7]. The area in green indicates the exposure of Mg-rich noritic anorthosite. (c) Iron abundance map derived from Kaguya MI data [12]. (d) Th abundance map obtained by [13].*

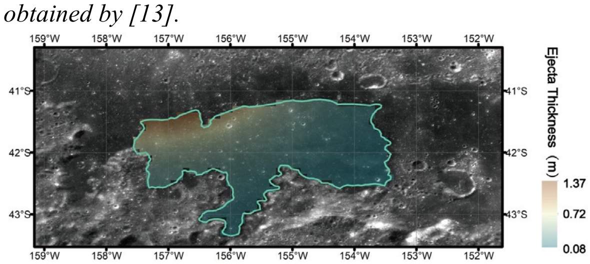

Fig 3. *Estimated ejecta thickness of Chaffee S in subregion F.*

We further assess the contribution of exotic materials from Chaffee S. Based on Pike's ejecta decay model [14], as shown in Fig. 3, the thickness of Chaffee S ejecta in subregion F may vary from ~8 cm to 1 m. The regolith gardening model [15] suggests that the top ~88.4 cm regolith in subregion F is mixed (by applying its age of 2.4 Ga). Assuming all ejecta from Chaffee S were mixed into the top regolith, the contribution of exotic materials from Chaffee S is at least 9%, comparable to the percentage of exotic materials in the CE-5 landing site [16].

Possible lithological types of CE-6 samples: On the basis of the above synthesis of CE-6 candidate landing sites (especially subregion F), we can make a preliminary prediction of the lithological types that CE-6 may sample in the future.

(a) Local mare basalts: CE-6 candidate landing sites are located within the mare/cryptomare regions. Thus, local mare/cryptomare basalts are likely to be the main lithological type in the collected samples. These first-sampled farside basalts will provide insight into the nature of the farside lunar mantle. Moreover, if some of the basalts is as young as the measurement from the CSFD analysis, why do they have different composition compared the nearside young Eratosthenian mare basalts represented by CE-5 (at least from the perspective of orbital remote sensing)? What is the heating source of the young farside mare basalts?

(b) Low-KREEP Mg-rich noritic material: This type of the lithology found in the CE-6 samples could be correlated with Mg-suite plutons in the local farside lower crust [8]. Considering that this deep-seated material may have undergone uplift to a shallower depth during the Apollo basin formation event and then excavated and exposed by subsequent post-Apollo impacts, perhaps it may aid in constraining the age of the Apollo basin. In addition, this low-KREEP Mg-suite lithology may also help clarify whether KREEP plays a pivotal role in Mg-suite petrogenesis during lunar secondary crust formation [17].

(c) KREEP-rich material: Moriarty et al. [18] pointed out that the Th-rich material within SPA originated from the SPA basin forming event. The Th-elevated feature of the Chaffee S ejecta suggests that such KREEP-rich SPA-related material may also be collected by CE-6. Using this material, the age of SPA basin is expected to be determined, which is crucial to understanding the early evolution of the Moon.

References: [1] Zeng et al. (2023) *Nat. Astron. 7(10),* 1188-1197. [2] Moriarty, D. P. & Pieters, C. M. (2018) *JGR: Planets, 123(3),* 729-747. [3] Barker, M. K. et al. (2016) *Icarus, 273,* 346-355. [4] Li, C. et al. (2018) *Geomatics Inf. Sci. Wuhan Univ., 43(4),* 485-495.[5] Baker, D. M. et al. (2011) *Icarus, 214(2),* 377-393. [6] Ivanov, M. A. (2018) *JGR: Planets, 123(10),* 2585-2612. [7] Petro, N. E. et al. (2010, March) *LPSC XLI*, Abst. #1533. [8] Wang et al. (2023) *Endurance Sci. Workshop*, Abst. #3043. [9] Wieczorek, M. A. et al. (2013) *Science, 339(6120),* 671-675. [10] Wang et al. (2023) *Endurance Sci. Workshop*, Abst. #3042. [11] Poehler, C. M. (2020) *EPSC 2020, Vol.14,* 600. [12] Lemelin, M. (2015) *JGR: Planets, 120(5),* 869–887. [13] Lawrence, D. J. (2003) *JGR: Planets, 108(E9),* 5102. [14] Pike, R. J. (1974) *EPSL, 23(3),* 265-271. [15] Costello, E.S. (2018) *Icarus, 314,* 327–344. [16] Qian et al. (2021), *EPSL, 561,* 116855. [17] Prissel, T. C. (2023) *Nat. Commun., 14(1),* 5002. [18] Moriarty III, D. P. (2021) *JGR: Planets, 126(1),* e2020JE006589.